

High-resolution structural study of Bi on Si(001)

G. E. Franklin*

Department of Physics, Harvard University, Cambridge, Massachusetts 02138

S. Tang†

*Department of Physics, Northwestern University, Evanston, Illinois 60208
and Materials Research Center, Northwestern University, Evanston, Illinois 60208*

J. C. Woicik

National Institute of Standards and Technology, Gaithersburg, Maryland 20899

M. J. Bedzyk

*Materials Research Center, Northwestern University, Evanston, Illinois 60208
and Materials Science Division, Argonne National Laboratory, Argonne, Illinois 60439*

A. J. Freeman

*Department of Physics, Northwestern University, Evanston, Illinois 60208
and Materials Research Center, Northwestern University, Evanston, Illinois 60208*

J. A. Golovchenko

*Department of Physics, Harvard University, Cambridge, Massachusetts 02138
and Rowland Institute for Science, Cambridge, Massachusetts 02142*

(Received 19 May 1995)

X-ray standing-wave measurements, along with first-principles local-density molecular-cluster calculations, have determined the Bi-dimer orientation, location, and bond length for the Si(001)-(1×2):Bi surface. The results for Bi directly scale with the covalent radii and with adsorption characteristics of other group-V elements (As and Sb) on Si(001).

The interaction of group-V adsorbates such as Sb and As with Si crystal surfaces has been the subject of both technological and fundamental surface science research in recent years.¹⁻⁷ Important benefits gleaned from this research include an improvement of the quality of III-V-compound epitaxial growth, delta doping, passivation, and surfactant-mediated growth of Ge overlayers on Si substrates.⁸⁻¹⁰ In contrast, very little work has focused on bismuth, the heaviest of the group-V elements.¹¹⁻¹⁶ Low-energy electron-diffraction (LEED) studies initially suggested that Bi adsorbs, at room temperature, as a disordered (1×1) array without breaking the underlying Si (2×1) reconstruction.¹² Recently, however, scanning tunneling microscopy (STM), LEED, and theoretical studies have indicated the existence of a Bi-dimer equilibrium structure which, at higher temperatures (>200 °C), produces (*n*×2) surface structures for coverages under a monolayer (1 ML)= 6.8×10^{14} atoms/cm².^{13,14,16} Here, mainly (1×2) and (2×2) reconstructed surfaces are observed. There is no consensus on the phase diagram of these structures, with (1×2), (2×2), and (*n*×2) occurring at various coverages and temperatures, but the basic building block seems to be the Bi dimer. Figure 1 shows two possible orientations (i.e., (a) perpendicular and (b) parallel to the [110] direction) for the Bi dimer sitting above the assumed bulklike Si(001) surface. This is also the direction for the clean Si(001) surface (2×1) dimer bond. The perpendicular Bi-dimer orientation is similar to that

found for Sb, where the dimers partially relieve the strain energy inherent in the buckled Si(001) clean-surface dimers.^{17,18} In addition, missing rows and antiphase boundaries, seen in STM topographs of both Sb and Bi on Si(001), also act to lower this strain energy.^{7,13,16,18}

This combined x-ray standing-wave (XSW) and first-

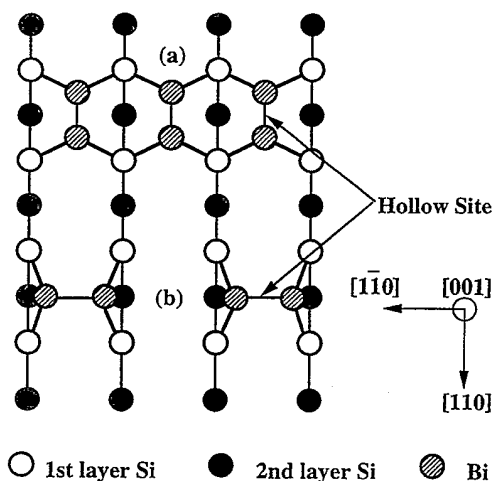


FIG. 1. Schematic drawing of two Bi-dimer structures on the Si(001) surface. Centered over the hollow sites are models for (a) the perpendicular dimer and (b) the parallel dimer.

principles local-density molecular-cluster (DMol) study focuses on samples that have been prepared at high temperature. From the x-ray standing-wave results the Bi-dimer bond length (L) and height (h') relative to the underlying bulk Si lattice for the $(n \times 2)$ structures have been determined. In addition, from the DMol calculations, it was found that the Bi dimers align perpendicular to the clean-surface Si-dimer direction. These results, scaled to the appropriate atomic sizes, are similar to previous XSW work performed on the Si(001)- (1×2) reconstructed surfaces of the other group-V elements, As (Ref. 1) and Sb.⁶

The x-ray standing-wave experiments were performed at the X15A beamline at the National Synchrotron Light Source at Brookhaven National Laboratory. Polished and Shiraki-etched Si(001) samples were inserted into our ultrahigh-vacuum (UHV) system, with a base pressure of 1.1×10^{-8} Pa. Each sample was flashed at 925 °C to remove the thin protective oxide layer. After cooling, LEED examination showed a two-domain (2×1) pattern characteristic of a clean Si(001) surface. Auger-electron spectroscopy found the sample to be free of carbon and oxygen. Approximately 3 ML (as determined from a quartz-crystal microbalance) of Bi were deposited from a degassed effusion cell onto a sample that was held at 400 °C. The sample was then annealed for 15 min at 500 °C to desorb excess Bi and enhance the interfacial order. From a separate calibrated Auger experiment, the saturation coverage was estimated to be about 0.7 ML. At ~ 50 °C above this temperature, Auger determined that all of the Bi had desorbed from the Si surface. Our procedure re-

producibly produced a two-domain (1×2) LEED pattern with fainter, smeared n th-ordered spots, similar to those reported previously.¹¹

The x-ray measurements were performed at an incident energy of 18.0 keV for both the Si(004) and Si(022) reflections while the sample was at room temperature. Whenever a new sample was prepared, standing-wave measurements were immediately recorded for both of these reflections. Figure 2 shows the measured (004) and (022) reflectivities as open squares and the corresponding Bi $L\alpha$ normalized fluorescence yields as open circles. The solid lines are the best fits calculated using dynamical diffraction theory. The two independent fitting parameters for each reflection, P_H and f_H , are called the coherent position and coherent fraction, respectively. These parameters are the amplitude (f_H) and phase (P_H) of the H th Fourier coefficient for the fluorescence-selected atom distribution. For a review of the XSW procedure and analysis, see Ref. 19.

The XSW coherent positions and coherent fractions for the (004) and (022) scans are $P_{004} = 1.27 \pm 0.01$, $f_{004} = 0.79 \pm 0.02$, $P_{022} = 1.15 \pm 0.01$, and $f_{022} = 0.66 \pm 0.02$. These values (within uncertainty) were also reproducibly found for coverages as low as 0.07 ML. From Fig. 3 we can see the relevant geometry where the Si bulk and surface atoms (open and gray-shaded circles) and the Bi atoms (filled circles) are shown in a projected view. The measured height above the top Si(004) bulklike atomic plane is then $h' = P_{004}d_{004} = 1.73 \pm 0.01$ Å. If we assume that the Bi dimers were centered above one of the hollow sites (see Figs. 1 and 3), then it can easily be proven that $P_{022} = (1 + P_{004})/2$. Our measured values for the coherent positions agree with this assumption. It should be noted that, from the point of view of the standing wave, both Bi-dimer domains on the Si(001) surface are identical.

In a general XSW analysis, the measured coherent frac-

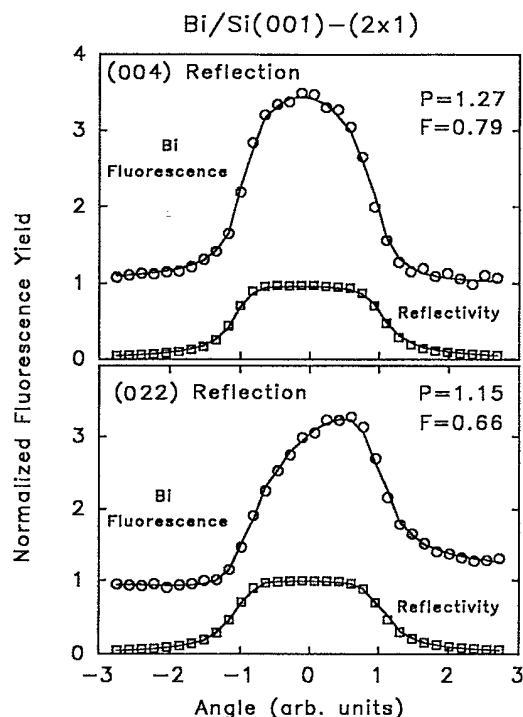


FIG. 2. The room-temperature measured (004) and (022) reflectivities (open squares) and the corresponding Bi $L\alpha$ normalized fluorescence yields (open circles) for the saturation coverage of Bi/Si(001). The solid lines are best fits to the data using dynamical diffraction theory. The coherent position (P) and coherent fraction (F) are the two independent fitting parameters.

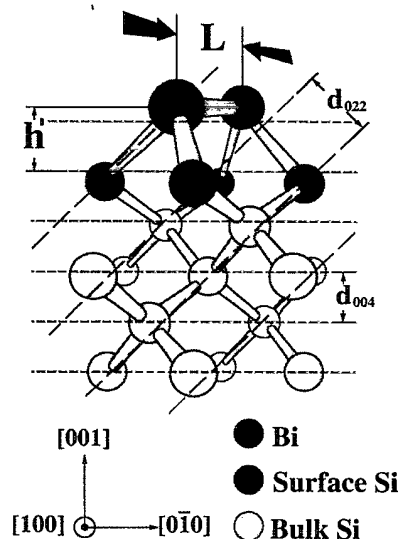


FIG. 3. Side view of the projected Bi dimer (filled circles), with bond length L , sitting atop surface and bulk Si atoms (gray-shaded and open circles). The size of the circles are indicative of the different Si layers going into the page and away from the viewer. Shown are the relevant lattice spacings d for the (004) and (022) reflections.

TABLE I. The covalent radii, dimer bond lengths (L), and dimer positions (h') above the top, unrelaxed Si(001) atomic plane are directly compared for various group-V elements. The bond lengths and positions were taken from previous XSW measurements for an accurate comparison.

Element	Covalent radii (Å)	L (Å)	h' (Å)
As (Ref. 1)	1.20	2.58 ± 0.04	1.40 ± 0.01
Sb (Ref. 6)	1.40	2.81 ± 0.09	1.64 ± 0.02
Bi	1.46	2.94 ± 0.06	1.73 ± 0.01

tion $f_{\mathbf{H}} = C a_{\mathbf{H}} D_{\mathbf{H}}$, where C (ordered fraction), $a_{\mathbf{H}}$ (geometrical factor), and $D_{\mathbf{H}}$ (Debye-Waller factor) are the three contributing factors. We have used the simplifying assumption that, for a given \mathbf{H} direction (with spacing d), $\langle u^2 \rangle$ is isotropic for each atom in the unit cell so that $D_{\mathbf{H}} = \exp(-2\pi^2 \langle u^2 \rangle / d^2)$. Since $a_{004} = 1$ for perfectly symmetric Bi dimers and $f_{004} = 0.79$, then $CD_{004} = 0.79$. From STM studies^{13,16} it seems clear that the Bi dimerized surface has many antiphase domains and missing-row defects. However, most Bi atoms seem to form ordered symmetric dimers within the long-range ($n \times 2$) order and therefore we assume $C = 1$. We note that STM images of Sb/Si(001) also show very similar highly ordered symmetric dimers amid antiphase domains and missing-row defects.^{7,18} We thus obtain, from D_{004} , a room-temperature root-mean-square thermal displacement, $\sqrt{\langle u_{004}^2 \rangle} = 0.15$ Å. We emphasize that we were able to get excellent fits (see Fig. 2) that required no inclusion of disorder. This thermal amplitude is close to 0.14 Å, a value established for As (Ref. 1) and Ga (Ref. 20) adsorbed dimers on the Si(001) surface.

In a similar analysis to that presented for the As,¹ Sb,⁶ Ge,²¹ and Ga (Ref. 22) dimers on Si(001), we determined from a_{022} the Bi-dimer bond length $L = 2.94 \pm 0.06$ Å. In the calculation for the bond length we assumed $C = 1$ and $\sqrt{\langle u_{022}^2 \rangle} = \sqrt{\langle u_{004}^2 \rangle} = 0.15$ Å (including a reasonable uncertainty estimate of ± 0.02 Å). This result is very close to the sum of two Bi covalent radii (2.92 Å). In Table I we have compared our values for the dimer bond length and position to other XSW results for As and Sb dimerized Si(001) surfaces. As can be seen from the table, there is an excellent correlation between the covalent radii of these elements and their dimer bond lengths and positions above the ideal Si(001) surface. This is compelling evidence, indicating that, despite differing amounts of induced surface strain, the fundamental bonding mechanisms are the same between different group-V elements and the Si(001) surface.

Total-energy and atomic-force calculations^{23,24} were performed using the DMol molecular-cluster approach to solve the local-density equations with the Hedin-Lundqvist exchange-correlation potential.²⁵ Cluster models ranging from 33 to 85 atoms were chosen to simulate the adsorption sites in question. The frozen-core approximation was made for Si and Bi except that the semicore Bi 5*d* electrons were treated fully in the self-consistent iterations. An extended double basis set was chosen for the Si and Bi atoms that contains a double set of valence functions plus a single polarization function.

A previous theoretical study¹⁴ showed that Si dimers on Si(001)-(2×1) were broken, and the Si(001)-(1×1) struc-

TABLE II. The calculated adsorption energy E_{adsor} (in eV/atom), the Bi-Bi bond length $L_{\text{Bi-Bi}}$ (in Å), and the Bi-dimer height h (in Å), above the Si(001) for the perpendicular and parallel dimer models displayed in Fig. 1 without Si substrate relaxation.

	Perpendicular	Parallel
E_{adsor} (eV)	-5.39	-4.07
$L_{\text{Bi-Bi}}$ (Å)	3.21	4.60
h (Å)	1.88	1.86

ture recovered, as a result of Bi adsorption at high coverage. Thus we only considered Bi adsorption on the Si(001) ideal surface and studied the two Bi-dimer adsorption configurations shown in Fig. 1. The mass center of the two dimers is at the fourfold hollow site with one having the dimer bond perpendicular and one parallel to the [110] direction. This is the Si-dimer bond direction in the Si(001)-(2×1) reconstructed surface. Without considering the Si substrate relaxation, we initially optimized the Bi-dimer bond length and height above the Si surface using a 33-atom cluster.²⁶

These results are presented in Table II, along with the adsorption energies calculated by subtracting the binding energy of the cluster without Bi from the binding energy of the cluster with Bi. The lower the adsorption energy (i.e., larger negative number), the more stable the adsorption system. From Table II, the parallel dimer model can be ruled out based on the following facts: (1) the parallel dimer has a higher adsorption energy than the perpendicular dimer, and (2) the sum of two Bi covalent radii (2.92 Å) is much closer to the perpendicular dimer bond length (3.21 Å) than to the parallel dimer bond length (4.60 Å).

With this structure as a starting point, a more realistic simulation, including relaxation of the Si lattice, was carried out. An 85-atom cluster consisting of five layers of Si (see Fig. 4) was allowed to relax. Si atoms up to the third layer were relaxed during which time the Bi dimer was kept sym-

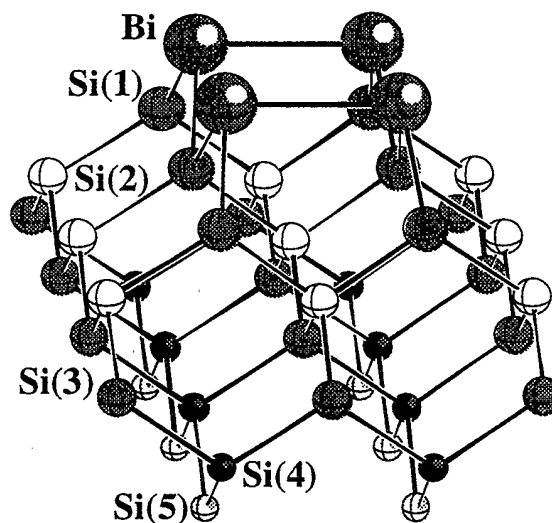


FIG. 4. $\text{Bi}_4\text{Si}_{41}\text{H}_{40}$ cluster models used in the calculation to simulate the symmetric Bi-dimer structure on Si(001). The H atoms are not shown in the figure.

TABLE III. Optimized structural parameters for the Bi perpendicular dimer on Si(001): $L_{\text{Bi-Bi}}$ and $L_{\text{Bi-Si}}$ stand for the bond length of the Bi dimer and Bi-Si, respectively; h' is the Bi-dimer height relative to the unrelaxed Si(001) surface plane; Δz represents the amplitude of inward relaxation of the first-layer Si atoms.

	DMol	XSW
h' (Å)	1.80	1.73 ± 0.01
$L_{\text{Bi-Bi}}$ (Å)	3.16	2.94 ± 0.06
$L_{\text{Bi-Si}}$ (Å)	2.68	
Δz (Å)	0.05	

metric. The results for the final optimized structure are listed in Table III along with our XSW measurements. It can be seen from the table that the calculated height of the Bi dimer and the Bi-Bi dimer bond length are in reasonable agreement with the experimental results. This confirms the validity of the perpendicular dimer structure predicted by the DMol calculations.

In addition to Table I, the theoretical results also suggest that Bi has a very similar behavior to other group-V metals (As and Sb) adsorbed on Si(001).²⁶ For example, they each adsorb in dimer form and with a dimer bond direction perpendicular to the Si-dimer bond on the clean Si(001)-(2×1) surface. The theoretical Bi-induced Si first-layer inward relaxation (0.05 Å) is the same as that for Sb/Si(001),²⁷ but slightly larger than that for As/Si(001) (0.03 Å).²⁷ How-

ever, because of the larger atomic size of Bi as compared with As, Bi atoms (like Sb) could induce larger stresses/strains on Si(001) and hence result in more defects or missing dimers, etc., on the surface. This was shown to be true in our experiment where the Bi-saturation coverage is only around 0.7 ML. The Sb- and As-saturation coverages are about 0.6–0.9 ML (Refs. 7 and 18) and 1 ML,²⁸ respectively.

We have performed room-temperature XSW measurements on the Bi-saturated Si(001) surface and found that the Bi dimers are located 1.73 ± 0.01 Å above the Si(004) bulk-extrapolated atomic plane and have a bond length of 2.94 ± 0.06 Å. Local-density calculations are in reasonable agreement with our experimental results and predict that the Bi dimers are oriented perpendicular to the Si-dimer bond direction on the Si(001)-(2×1) reconstructed surface. Finally, the results for Bi are similar to those for As and Sb and directly scale with their covalent radii.

The experimental work was supported by the U.S. Department of Energy under Contract No. DEFG02-89ER-45399 to Harvard University, under Contract No. W-31-109-ENG-38 to Argonne National Laboratory, and under Contract No. DE-AC02-76CH00016 to the facilities of the NSLS at Brookhaven National Laboratory. The theoretical work was supported by the MRL Program of the National Science Foundation, at the Materials Research Center of Northwestern University, under Award No. DMR-9120521, and by a computing grant from the National Center for Supercomputing Applications, Urbana-Champaign, Illinois.

*Present address: Sandia National Laboratory, Department of Surface and Interface Science, Albuquerque, NM 87185.

†Present address: Texas Instruments, Inc., Central Research Laboratories, MS 147, Dallas, TX 75265.

¹G. E. Franklin, E. Fontes, Y. Qian, M. J. Bedzyk, J. A. Golovchenko, and J. R. Patel, Phys. Rev. B **50**, 7483 (1994).

²R. I. G. Uhrberg, R. D. Bringans, R. Z. Bachrach, and J. E. Northrup, Phys. Rev. Lett. **56**, 520 (1986).

³S. Tang and A. J. Freeman, Phys. Rev. B **48**, 8086 (1993).

⁴D. H. Rich, F. M. Leibsle, A. Samsavar, E. S. Hirschorn, T. Miller, and T.-C. Chiang, Phys. Rev. B **39**, 12 758 (1989).

⁵D. H. Rich, T. Miller, G. E. Franklin, and T.-C. Chiang, Phys. Rev. B **39**, 1438 (1989).

⁶P. F. Lyman, Y. Qian, and M. J. Bedzyk, Surf. Sci. **325**, L385 (1995).

⁷M. Richter, J. C. Woicik, J. Nogami, P. Pianetta, K. E. Miyano, A. A. Baski, T. Kendlewicz, C. E. Bouldin, W. E. Spicer, C. F. Quate, and I. Lindau, Phys. Rev. Lett. **65**, 3417 (1990).

⁸D. H. Rich, A. Samsavar, F. M. Leibsle, and T.-C. Chiang, Phys. Rev. B **40**, 3469 (1989).

⁹G. E. Franklin, D. H. Rich, H. Hong, T. Miller, and T.-C. Chiang, Phys. Rev. B **45**, 3426 (1992).

¹⁰M. Horn-von Hoegen, F. K. LeGoues, M. Copel, M. C. Reuter, and R. M. Tromp, Phys. Rev. Lett. **67**, 1130 (1991).

¹¹T. Hanada and M. Kawai, Surf. Sci. **242**, 137 (1991).

¹²W. C. Fan, N. J. Wu, and A. Ignatiev, Phys. Rev. B **45**, 14 167 (1992).

¹³C. Park, R. Bakhtizin, T. Hashizume, and T. Sakurai, Jpn. J. Appl. Phys. **32**, L528 (1993).

¹⁴S. Tang and A. J. Freeman, Phys. Rev. B **50**, 1701 (1994).

¹⁵K. Sakamoto, K. Kyoya, K. Miki, and H. Matsuhata, Jpn. J. Appl. Phys. **32**, L204 (1993).

¹⁶H. P. Noh, Ch. Park, D. Jean, K. Cho, T. Hashizume, Y. Kuk, and T. Sakurai, J. Vac. Sci. Technol. B **12**, 2097 (1994).

¹⁷R. A. Wolkow, Phys. Rev. Lett. **68**, 2636 (1992).

¹⁸J. Nogami, A. A. Baski, and C. F. Quate, Appl. Phys. Lett. **58**, 475 (1991).

¹⁹J. Zegenhagen, Surf. Sci. Rep. **18**, 199 (1993).

²⁰Y. Qian and M. J. Bedzyk, J. Vac. Sci. Technol. A **13**, 1613 (1995).

²¹E. Fontes, J. R. Patel, and F. Comin, Phys. Rev. Lett. **70**, 2790 (1993).

²²Y. Qian, M. J. Bedzyk, S. Tang, A. J. Freeman, and G. E. Franklin, Phys. Rev. Lett. **73**, 1521 (1994).

²³B. Delley, J. Chem. Phys. **92**, 508 (1990), and references therein.

²⁴B. Delley, J. Chem. Phys. **94**, 7245 (1991).

²⁵L. Hedin and B. I. Lundqvist, J. Phys. C **4**, 2064 (1971).

²⁶See Fig. 4 in S. Tang and A. J. Freeman, Phys. Rev. B **48**, 8068 (1993).

²⁷S. Tang and A. J. Freeman (unpublished); (private communication).

²⁸R. S. Becker, T. Klitsner, and J. V. Vickers, J. Microsc. **152**, 157 (1988).